Int. J. Heat Mass Transfer. Vol. 24, No. 4, pp. 671–683, 1981
Printed in Great Britain

0017–9310/81/040671–13 $02.00/0

A MATHEMATICAL MODEL OF A RAMP FORCED HOT-WIRE THERMAL CONDUCTIVITY INSTRUMENT

SHAMSEDDIN S. MOHAMMADI, MICHAEL S. GRABOSKI* and E. DENDY SLOAN
Department of Chemical and Petroleum-Refining Engineering,
Colorado School of Mines, Golden, CO 80401, U.S.A.

(*Received* 9 *June* 1980 *and in revised form* 29 *September* 1980)

Abstract — The fundamental model and model corrections for the absolute determination of fluid thermal conductivity using a transient hot-wire technique were studied. Analytical solutions for three heat generation functions (Dirac, step and ramp) are presented. The ramp heat generation function is shown to offer several advantages over the step function, which is currently used by experimenters. Expressions for the corrections to the idealized model of a ramp forced system are presented for: heat capacity effect, truncation error, non-uniform wire radius, bounded media, Knudsen effects, axial conduction, free convection and radiation.

NOMENCLATURE

A, ratio of radiative to conductive heat flux;
b, outer cell radius [m];
C_p, specific heat [$W s kg^{-1} K^{-1}$];
C, $\exp(\gamma)$;
D, $\exp(1+\gamma)$;
E, characteristic dimension;
E_1, exponential integral;
g, gravitational acceleration [$m s^{-2}$];
J_0, Bessel function;
H_0, interfacial conductance coefficient [$W m^{-2} K^{-1}$];
H, $(H_0 P/\pi k)$;
$I_\S$, black body radiation intensity;
k, thermal conductivity [$W m^{-1} K^{-1}$];
K_a, mean extinction coefficient;
L, wire length [m];
O, accumulation of high-order terms;
P, wire perimeter $(2\pi r_w)$ [m];
q, heat flux [$W m^{-1}$];
$\hat{q}$, heat content of a pulse;
$\dot{q}$, slope of the ramp [$W m^{-1} s^{-1}$];
Q, $q/(\pi k T_0)$;
$\bar{Q}$, $\dot{q} r_w^2/k T_0$;
r, radial position;
r_w, wire radius [m];
R, (r/r_w);
S, area (πr_w^2) [m^2];
t, time [s];
T, temperature [K];
u, axial velocity [$m s^{-1}$];
U, $u r_w/v$;
v, radial velocity [$m s^{-1}$];
V, $v r_w/v$;
Y_0, Bessel function;
z, axial position;
Z, z/r_w;
BU, Bouguer number, κr_w;
Pr, Prandtl number;
Gr, Grashof number, $[g\beta r_w^3 T_0/v^2]$;
§, frequency.

Greek symbols

α, thermal diffusivity [$m^2 s^{-1}$];
β, thermal expansion coefficient [K^{-1}];
γ, Euler's constant (0.5772);
δ, difference;
δ_t, thermal boundary layer thickness [m];
Δ, difference;
ε, emissivity;
ρ, density [$kg m^{-3}$];
Λ, mean free path;
ν, kinematic viscosity [$m^2 s^{-1}$];
μ, H/α;
σ, Stefan–Boltzman constant;
κ, absorption coefficient [m^{-1}];
τ, vt/r_w^2 (unless defined otherwise), for wire $\tau_w = \alpha_w t/r_w^2$;
$\bar{\tau}_0$, optical thickness;
θ, $(T - T_0)/T_0$;
Ψ, empirical factor;
ξ, numerical factor;
ϕ, numerical factor;
η, refractive index;

Superscripts

$^-$, average;
*, at the time of the onset of convection.

Subscripts

w, wire;
f, fluid;
0, initial;
r, radiative;
c, conductive.

1. INTRODUCTION

THE THERMAL conductivity of liquids and gases has proved to be one of the most difficult properties to

*The author to whom correspondence should be made.

predict and to measure. On a molecular scale, the thermal conductivity of polyatomic molecules differs from viscosity and diffusivity in that energy flux includes a contribution due to internal degrees of freedom as well as a contribution due to translational energy [1]. Past experimental determinations of thermal conductivity have been hindered by the onset of natural convection and radiation. Recently, however, a number of investigators [2–7] have made significant experimental progress through modifications of the transient hot-wire measurement technique.

Basically, the transient hot-wire method consists of imposing a heat generation function on a vertical wire which is immersed in a stationary cylinder containing the fluid of interest. The temperature change of the wire, ΔT_w which is a function of the heat conducted by the fluid, is measured as a function of time, t. The thermal conductivity of the fluid is then determined from the analytical solution of the partial differential equations describing the transient conduction phenomena in the system.

To date, only one heat generation function, the step function, has been extensively used. The use of the step function for heat generation necessitates very short experimental times, typically less than 2 s [2, 5, 6, 8], or for less accurate measurements, less than 20 s [7]. The short duration of the experiment has necessitated data acquisition equipment that is sophisticated and/or expensive. Other heat generation functions which may be used in transient thermal conductivity measurements include the Dirac and the ramp functions.

The Dirac function represents the simplest forcing function which may be employed. The short duration and the small amount of heat input to the system minimizes any contributions to the apparent thermal conductivity from convection and radiation. The major disadvantage of the Dirac input is the high speed the precise measurements require to deduce the thermal conductivity.

The ramp function possesses several unique qualities which make it useful for thermal conductivity measurements. Since the temperature rise of the wire is gradual, convective and radiative contributions to the apparent thermal conductivity may be greatly reduced in comparison to the step function. Furthermore, since the ramp forced system does not degenerate to a steady-state, longer experimental times are also possible. Accurate and precise generation of a ramp function as well as transient temperature measurements of the wire can be accomplished at relatively low cost.

Under a Department of Energy (DOE) sponsored research contract, a system for measuring the thermal conductivity of synthetic liquid fuels at a temperature range of 300–560 K and a pressure range of 1–100 atm has been designed and constructed. This system employs a ramp heat generation function. A brief description of the system, along with a sample test on liquid toluene is presented in order to illustrate the merits of the technique.

In this paper, we have mathematically investigated the above three forcing functions to determine which might be the most promising for transient analysis. It is concluded that the ramp function has several advantages as a forcing function. Based on this conclusion, a detailed analysis of a ramp perturbed system has been conducted to determine the deviations from the ideal mathematical model. These studies have been used to establish design criteria to minimize experimental error and provide a method for correcting the apparent thermal conductivity for the residual errors.

2. EXPERIMENTAL VERIFICATION

In the experimental technique employed by this group of investigators, a ramp power forcing function is used to heat a platinum wire ($r_w = 6.35\,\mu$m) 0.14 m long. The ramp is generated using a digital power supply controlled by a microcomputer. The wire resistance change is measured by a Wheatstone bridge and a series of amplifiers. Time measurements are made accurately by the computer crystal clock. A typical experiment requires 1–5 s and yields 1022 data points which are statistically analyzed to obtain the thermal conductivity based on the model presented in this paper.

From the mathematical model of the ideal line-source described in the forthcoming sections, it is apparent that a plot of θ/t vs $\ln(t)$ would result in a straight line with its slope proportional to the thermal conductivity of the fluid under consideration. Such a plot is presented in Fig. 1 which illustrates raw data for liquid toluene at 299.35 K. The apparent thermal conductivity value obtained over the time interval of 0.1–5 s is $0.126\,\mathrm{W\,m^{-1}\,K^{-1}}$ as compared to the corrected value of $0.129\,\mathrm{W\,m^{-1}\,K^{-1}}$ reported by Mani [9].

Experimental work is currently under way to achieve an accuracy of better than 2% in the thermal conductivity measurement.

3. THEORY OF THE TRANSIENT HOT-WIRE TECHNIQUE

The transient hot-wire cell consists of an electrically heated fine wire suspended vertically in the fluid medium for which thermal conductivity is to be measured. The fluid is contained in a cylindrical enclosure and maintained initially at a constant temperature. The transient behavior of this hot wire is idealized by the solution of the transient one-dimensional pure conduction problem involving an infinitely long line source subjected to a time variant perturbation situated in an isotropic fluid, infinite in extent and initially in local thermodynamic equilibrium.

3.1. *Ideal mathematical model*

The simplest mathematical description of the non-

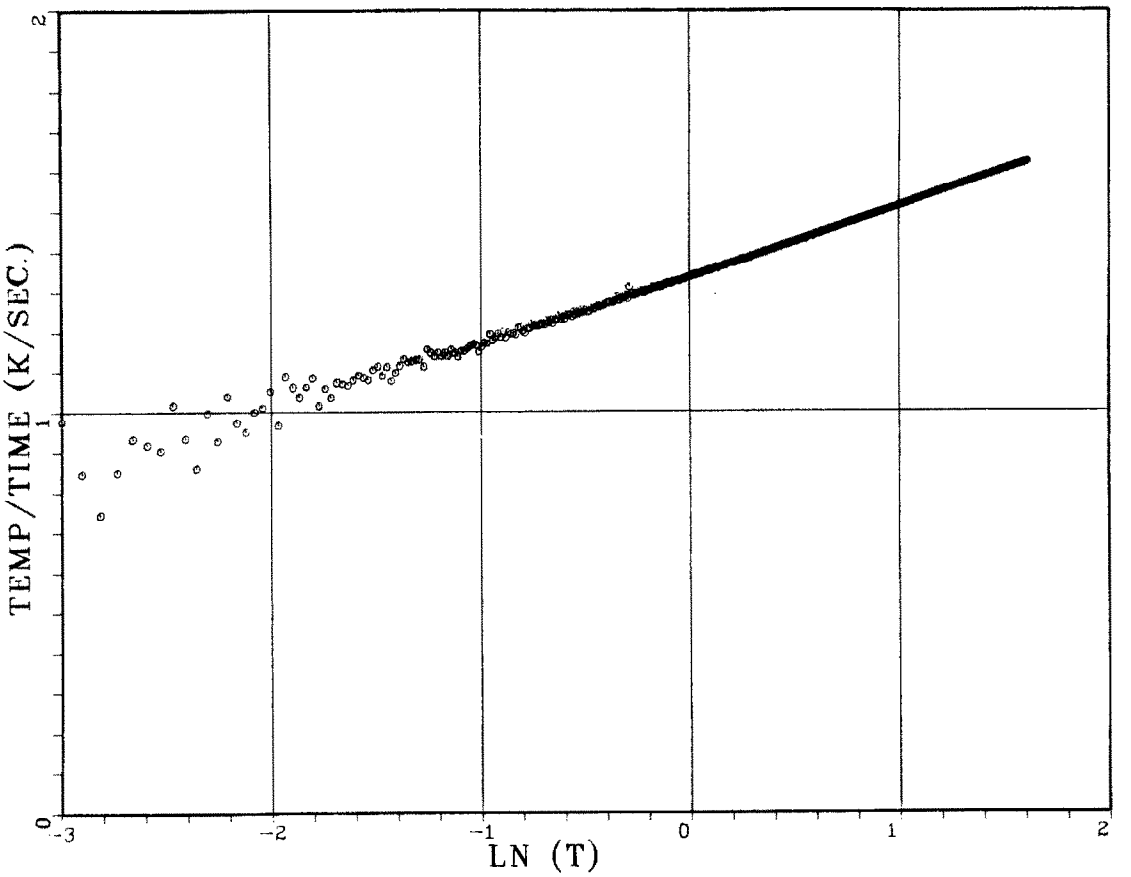

FIG. 1. Experimental values of transient temperature rise for liquid toluene at 299.35 K in a ramp forced thermal conductivity instrument.

steady-state hot-wire cell is given by the line-source solution of the conduction equation

$$\frac{\partial T}{\partial t} = \alpha\left[\frac{\partial^2 T}{\partial r^2} + \frac{1}{r}\frac{\partial T}{\partial r}\right] \tag{1}$$

I.C. $T(r,0) = T_0$

B.C. (1) $\lim_{r\to\infty} T(r,t) = T_0$

(2) $-2\pi r k_f \left.\frac{\partial T}{\partial r}\right|_{r\to r_w} = q(t).$

The input function $q(t)$ represents the rate of heat per unit length of wire. The general solution to any forcing function may be written in general terms using the convolution integral theorem as

$$T(r,t) - T_0 = \frac{1}{4\pi k_f}\int_0^t q(t-u)\exp\left(\frac{-r^2}{4\alpha t}\right)\frac{du}{u} \tag{2}$$

3.1.1. *Dirac function.* For the Dirac function $q(t-u) = \mathring{q}(t-u)$ where $\mathring{q}$ represents the heat content of the pulse. The solution is

$$T(r,t) - T_0 = \frac{\mathring{q}}{4\pi k_f t}\exp\left(\frac{-r^2}{4\alpha t}\right). \tag{3}$$

For large t:
and small r: $$T(r,t) - T_0 = \mathring{q}/4\pi k_f t. \tag{4}$$

For the Dirac function, the solution shows that at any fixed radial coordinate the thermal conductivity may be determined from the slope of a plot of ΔT vs $1/t$ when t is large (exponential goes to unity) provided $\mathring{q}$ is known. Thus, for large times the straight line may be used to deduce the thermal conductivity and also as a criteria for the conformance of the system and model.

3.1.2. *Step function.* For the step function $q(t-u) = q$. The magnitude of the step is represented by q. The well-known solution (10) is therefore

$$T(r,t) - T_0 = \frac{q}{4\pi k_f} E_1\left(\frac{r^2}{4\alpha t}\right) \tag{5}$$

where E_1 represents the first exponential integral.

$$E_1(u) = \int_u^\infty e^{-u}\frac{du}{u}. \tag{6}$$

For long times, the first exponential integral may be expanded and the series truncated.

$$E_1(r^2/4\alpha t) = -\gamma + \ln\left(\frac{4\alpha t}{r^2}\right) + \left(\frac{r^2}{4\alpha t}\right) + O\left[\frac{r^2}{4\alpha t}\right]^2 \tag{7}$$

where O represents the accumulation of higher-order terms. The resulting solution for long times is

$$T(r,t) - T_0 = \frac{q}{4\pi k_f} \ln\left(\frac{4\alpha t}{r^2 c}\right). \quad (8)$$

In the case of the step function, a plot of ΔT against $\ln t$ provides a method of establishing the thermal conductivity based on a knowledge of q.

3.1.3. *Ramp function.* For the ramp function, $q(t-u) = \hat{q}(t-u)$. In this case $\hat{q}$ represents the slope of the ramp. The convolution integral gives the following solution

$$T(r,t) - T_0 = \frac{\hat{q}t}{4\pi k_f}\left[E_1\left(\frac{r^2}{4\alpha t}\right) - \exp(-r^2/4\alpha t) + \left(\frac{r^2}{4\alpha t}\right)E_1\left(\frac{r^2}{4\alpha t}\right)\right]. \quad (9)$$

As in the previous cases, the solution may be simplified for long times to give

$$\frac{T(r,t) - T_0}{t} = \frac{\hat{q}}{4\pi k_f} \ln\left(\frac{4\alpha t}{r^2 D}\right). \quad (10)$$

For the ramp function, a plot $\Delta T/t$ against $\ln t$ provides the criteria for establishing k_f.

3.2. *Discussion of experimental methods*

Each of the forcing functions considered has some potential merit for measuring thermal conductivities of fluids. However, each also presents experimental difficulties.

3.2.1. *Dirac function.* The Dirac function represents the simplest forcing function which may be employed. Based on current electronics, there is no extreme difficulty involved in generating this function with extreme precision for modest power levels. In principle, the Dirac function has a number of important advantages: firstly, the heat input to the system is small, thus free convection and radiation effects are insignificant; secondly, the duration of the experiment is such that many experiments can be run within a short time.

A major disadvantage of the Dirac input involves the measurements required to deduce the thermal conductivity. At the moderate power levels used in solid-state circuits, the maximum temperature rise which occurs in a typical cell is on the order of 0.05 to 0.5 K; this rise occurs at times of the order of 0.01 ms. For times when the temperature–time response may be plotted in a linear fashion, the observed ΔT estimated from the simple model is on the order of 10^{-1}–10^{-5} K and occurs between 1 and 100 ms for most fluids. Table 1 presents some calculations for nitrogen and toluene using the Dirac function.

The inability to accurately measure the small ΔT responses will limit the accuracy of the thermal conductivity which may be obtained using the pulse.

3.2.2. *Step function.* The step function has been employed by the previous researchers for both gas and liquid thermal conductivity measurements. Application of this model represents the state of the art in thermal conductivity measurements. Many of the correction factors for the additional heat transfer contributions to the apparent thermal conductivity are presented by McLaughlin and Pittman [11], and by Healy *et al.* [12].

The step function has several limitations which restrict its usefulness. In the application of the step input, the system is strongly perturbed at short times. The majority of the temperature increase takes place at very short times and is not useful in the analysis. For a typical power input, and a cell wire-resistance of 100 Ω, Table 2 indicates the temperature rise as a function of time. The lower time represents the initiation of the linear portion of the ΔT–$\ln t$ plot while the upper time represents the time of departure from linearity due to the onset of steady-state. The total resistance change is 0.20 Ω over the useful range of the experiment even though the total resistance increase is on the order of 0.53 Ω. Thus, less than 40% of the total resistance increase is used in the measurement. If the sensitivity is to be improved, a higher power level should be employed. However, this will create a larger initial temperature rise and increase the effect of natural convection and radiation on the heat transfer from the wire surface. Sensitivity may also be increased somewhat by going to thinner wires for which the resistance per unit length is greater.

At longer times, the onset of steady-state limits the duration of the experiment. For gases, this is important as this time is generally on the order of 600 ms. For liquids, the time is much longer and generally does not represent a limitation of the technique.

3.2.3. *Ramp function.* The ramp function possesses several unique qualities which make it useful for thermal conductivity measurements. The only major drawback to its use is the requirement of a precision function generator capable of producing a current which varies as the square root of time. However, highly accurate generators may be readily constructed using solid-state electronics.

In employing the ramp function, the power level increases with time. Thus, at short times when the model equation cannot be plotted in a linear fashion,

Table 1. Typical operation of a hot-wire thermal conductivity for several fluids using a Dirac input

ΔT, K, wire surface	Time, ms
Nitrogen (gas), 1 MPa, 289 K	
1.82*	0.003
0.014	1
0.0014	10
0.00014	100
Toluene (liquid), 0.1 MPa, 289 K	
0.013*	0.08
0.003	1
0.0003	10
0.00003	100

*Maximum temperature.

Table 2. Typical operating data for a step input for toluene at ambient ($q = 0.320\ \mathrm{W\,m^{-1}}$)

Time, ms	ΔT, K	ΔR, Ω
100	1.23	0.325
300	1.45	0.383
600	1.58	0.418
1000	1.69	0.447
2500	1.87	0.494
4000	1.96	0.518
5000	2.01	0.531

the power level is low and the temperature rise is small. Additionally, the ultimate temperature rise and experiment duration may be controlled by varying both the power level applied to the ramp generator and the gain, thus permitting free convection and radiation effects to be minimized or eliminated. Since the ramp forced system does not degenerate to a steady-state, longer experimental times are also possible.

This may simplify the time measurement significantly. Table 3 presents typical operating data for a ramp input for toluene. At short times during the initial stabilization of the measuring circuit (in the order of 60–100 ms) only 12% of the overall resistance change occurs; the remaining 88% can be utilized for the thermal conductivity measurement.

Therefore, the ramp heat perturbation has significant advantages over the Dirac and step functions and the remainder of this paper will deal only with this type of heat generation function.

4. ANALYSIS OF APPROXIMATIONS TO THE IDEAL LINE-SOURCE MODEL FOR RAMP PERTURBATION

The ideal line-source model only approximates the response of the actual cell. A variety of factors which might effect the temperature response of the wire must be considered.

4.1. *Truncation error*

This error arises from the truncation of the $E_1(u)$ to obtain the long time solution. The ideal line-source solution given by equation (10) is

$$\frac{\Delta T}{t} = \frac{\hat{q}}{4\pi k_f}\left[E_1\left(\frac{1}{4\tau}\right) - \mathrm{e}^{-(1/4\tau)} + \left(\frac{1}{4\tau}\right)E_1\left(\frac{1}{4\tau}\right)\right] \tag{11}$$

where

$$Ei\left(\frac{1}{4\tau}\right) = -\gamma + \ln(4\tau) + \frac{1}{4\tau} + O\left[\left(\frac{1}{4\tau}\right)^2\right] \tag{12}$$

O represents the accumulation of higher-order terms, and $\tau = \alpha t/r_w^2 D$.

For very thin wires the terms in equation (12) of order $(1/\tau)^2$ and smaller may be ignored. Substituting the above expression into equation (11) and comparing with the long time solution yields the following equation for truncation error

$$\frac{\delta\Delta T}{\Delta T} = \left(\frac{1}{4\tau}\right)\left(2 + \ln\left(\frac{4\tau}{D}\right)\right) + 1 - \mathrm{e}^{-(1/4\tau)}/\ln\left(\frac{4\tau}{D}\right). \tag{13}$$

At ambient conditions, using a wire with a radius of 6.35 μm, for a typical case of methane at time 100 ms, the truncation error equals 3.6×10^{-2}%. For toluene under similar conditions, the error is about 0.25%. Since the error is inversely proportional to time, a starting time may be selected for which the truncation error is insignificant.

4.2. *Non-uniform wire radius*

Considering the ideal line-source solution for a ramp forcing function [i.e. equation (10)], as long as the rate of energy supply per unit length remains the same, the temperature history at any given radial position in the fluid is independent of the radius of the wire. Following Healy [12] we conclude that the thermal conductivity can therefore be estimated at $r \to r_w$, without expending much effort to insure accurate cylindricity of the wire. It should be noted that periodic fluctuations in the wire radius on a scale comparable to the wire radius may contribute to deviations from the ideal line source. The magnitude of this deviation cannot be readily predicted, since the conductive boundary condition contains a varying flux angle. In practice the wire should be examined optically to assure uniform cylindricity. Very uniform drawn wire with a radius of as little as 6.35 μm (1/2000″) can be obtained from commercial suppliers. The cell wire which is currently being used in this laboratory is of this type.

4.3. *The effect of finite wire heat capacity*

The transient one-dimensional equations of energy for the hot wire and the fluid surrounding it along with the appropriate boundary conditions are

$$\rho_w C_{pw}\left(\frac{\mathrm{d}T_w}{\mathrm{d}t}\right) = \frac{q}{\pi r_w^2} + \frac{k_f}{r_w}\left(\frac{\partial T}{\partial r}\right)_{r_w} \tag{14}$$

and

$$\rho_f C_{pf}\left(\frac{\partial T}{\partial t}\right) = k_f\left[\frac{\partial^2 T}{\partial r^2} + \frac{1}{r}\left(\frac{\partial T}{\partial r}\right)\right] \tag{15}$$

Table 3. Typical operating data for a ramp input for toluene at ambient ($\hat{q} = 0.071\ \mathrm{W\,m^{-1}\,s^{-1}}$)

Time, ms	ΔT, K	ΔR, Ω
100	0.023	0.006
300	0.083	0.022
600	0.184	0.049
1000	0.330	0.087
2500	0.924	0.224
4000	1.560	0.412
5000	2.000	0.528

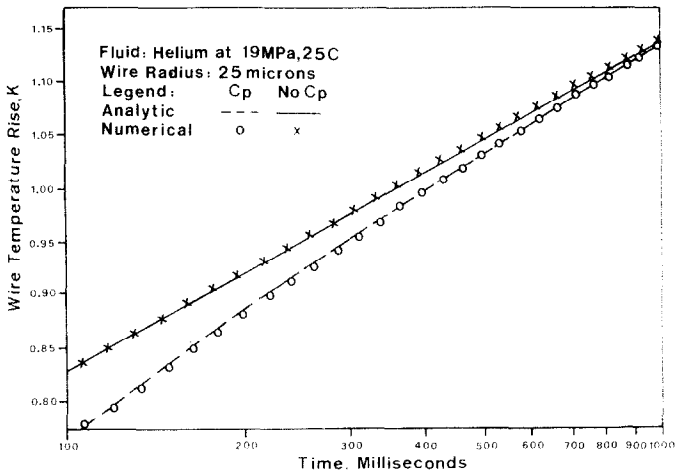

FIG. 2. Heat capacity effect on the numerical and analytical solutions of the transient one-dimensional conduction with a step change in heat flux.

with B.C.

$$t < 0 \qquad T_w = T = T_0$$

$$t \geqslant 0 \qquad r = \infty,\ T = T_0$$

$$t \geqslant 0 \qquad r = r_w,\ T_w = T$$

where subscripts w and f represent the wire and fluid, respectively.

Equations (14) and (15) were transformed to dimensionless groups and solved numerically. The space derivatives were approximated by a second-order correct Taylor series expansion about the center points, with the exception of the boundaries, where both forward and backward differences were applied. The tridiagonal matrix resulting from equation (15) was solved at each time interval using the Thomas algorithm. All implicit time derivatives were approximated to first-order accuracy, which necessitated relatively small time-steps.

The finite difference model solutions neglecting and considering wire heat capacity are shown to agree with the analytical solutions (10) in Fig. 2 for a step change of heat in a system using helium with the outer cell dimensions specified by DeGroot *et al.* [2]. For the purpose of testing the model, a wire of radius 25 μm was chosen. This size probably represents the largest wire size an experimenter would consider due to wire resistance considerations and, because of the wire mass, represents a case where the wire heat capacity effect is very important.

The finite difference model was also compared with the analytical solution for the ramp heat input function, neglecting wire heat capacity. Using a typical fluid, toluene, the numerical and the analytical solutions for the simple ideal line-source agree to within 1%. These solutions, therefore, bracket all situations of importance. The excellent agreement suggests the numerical model is generally applicable.

The finite difference model was used to investigate the wire heat capacity effect for a ramp heat input function. Using toluene, the heat capacity effect is undetectable for a wire with a diameter of 5 μm when the heat is input at a typical experimental rate of 0.0283 W m^{-1} s^{-1}. For the same heat input, but with an order of magnitude larger wire, the heat capacity effect causes about 2% error in the slope of $\Delta T/t$ vs $\ln(t)$ plot. For modest wire diameters, the wire heat capacity effects are large at short times but decrease rapidly as time progresses. Figure 3 illustrates the time-dependent nature of the heat capacity induced error for liquid toluene. Finally, it should be noted that the ratio of the product of the density and the heat capacity of the fluid to that of the wire (i.e. $\omega = \rho_f C_f/\rho_w C_w$) is the controlling parameter in the generation of the error in thermal conductivity. If $\omega = 1$, then the effect of finite heat capacity is insignificant at all times. For liquid toluene ($\omega = 0.5$) the maximum value of the correction is 0.4% at $\tau = 950$, but for gases such as methane where ω can be as low as 0.05, the correction is in the order of 5–7%.

4.4. *Bounded media*

For a step heat generation function, McLaughlin and Pittman [11] have modified the boundary condition at the inner cell wall (i.e. at $r = b$, $T_f = T_0$) and have resolved the transient conduction equation. For $b/r_w \gg 1$ (b is the inner cell radius) the difference between the asymptotic form of the solution originally derived by Fischer [13], and the ideal line solution is obtained. Numerical solutions for various values of b/r_w and τ yield the percent error of the hot-wire temperature due to wall effect. Similar analysis by Healy *et al.* [12] resulted in a criterion for determination of the inner cell radius, based on minimization of the difference between the ideal line-source solution and the one from the modified

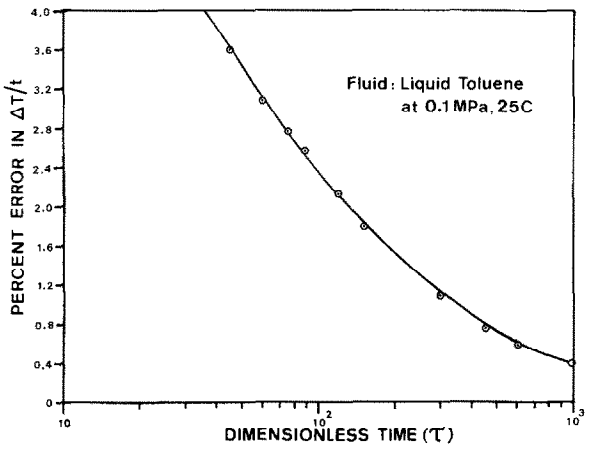

FIG. 3. Heat capacity effect for liquid toluene at ambient condition in a ramp forced system.

boundary case. This criteria ($b^2/\alpha t > 5.783$ ...) confirms the results of McLaughlin and Pittman [11]. Healy's method of solution is utilized for the case of ramp power generation input. Using Duhamel's integral technique [14], the temperature profile resulted from the modified boundary condition is obtained for the ramp perturbation as

$$\Delta T = \frac{\hat{q}}{4\pi k_f}\left[2t\ln\left(\frac{b}{r_w}\right) - \left[\sum_{n=1}^{\infty}\left(\frac{\pi Y_0(g_n)}{A}\right)(1-e^{-At})\right]\right] \tag{16}$$

where $A = g_n^2$; α/b^2, and g_n denote the roots of $J_0(g_n) = 0$ ($g_n = 2.4048, 5.5201, 8.6537, 11.7315, 14.9309\ldots$).

The solution of the ideal line-source can be rearranged as

$$\Delta T_{\text{I.D.}} = \frac{\hat{q}}{4\pi k_f}\left[2t\ln\left(\frac{b}{r_w}\right) + t\ln\left(\frac{4\alpha t}{b^2 D}\right)\right]. \tag{17}$$

Therefore, an outer-boundary correction can be obtained as

$$\delta\Delta T = \Delta T_{\text{I.D.}} - \Delta T = \frac{\hat{q}}{4\pi k_f}\left[t\ln\left(\frac{4\alpha t}{b^2 D}\right) + \sum_{n=1}^{\infty}\frac{\pi Y_0(g_n)}{A}(1-e^{-At})\right]. \tag{18}$$

By selecting an appropriate bound on the value of $b^2/\alpha t$ one can establish an order of magnitude limitation on $\delta\Delta T/\Delta T$, so that it contributes an error of 0.01% or less to thermal conductivity.

The numerical solution of the above equation, with Bessel functions generated from a polynomial approximation (15) and the roots of $J_0(g_n)$ taken from standard tables [16] for the first 50 terms, gave a criterion $b^2/\alpha t > 3.120$. This compares favorably with the value of $b^2/\alpha t = 5.783$ for the same error size with a step function. The experiment with the ramp input may be run almost twice as long as the step without the outer boundary correction. When the outer boundary correction is made, the size of the correction may be determined by equation (18).

4.5. *Knudsen effects*

Since very thin wires are employed to reduce the correction due to their finite heat capacity, it must be expected that Knudsen effects may be important at the lower densities where the mean free path in the gas becomes of the same order of magnitude as the wire diameter. For a uniform heat input to the wire Healy *et al.* [12] have shown that the principal effect, to the first order, is a shift in all points on the ΔT vs $\ln t$ diagram by a constant amount without changing the slope, i.e. the reported value of k_f. At lower densities, second-order corrections are more significant and need to be considered. For a typical case of helium at 1 atm and room temperature, Healy *et al.* [12] reported that the Knudsen effect results in a 0.3% error in k_f for a wire with $r = 2.5\ \mu$m.

The Smoluchowski equation (17) may be used to describe the difference in temperature between the fluid and wire due to Knudsen effect

$$T_w(r_w, t) - T(r_w, t) = -\psi\left(\frac{\partial T}{\partial r}\right)_{r=r_w}. \tag{19}$$

In equation (19) T_w is the wire temperature, T is the temperature of the adjacent gas and ψ is an empirical factor proportional to the mean free path of the gas. No reliable measurements of this factor are available. Using the following boundary condition

$$-2\pi r_w k_f\left(\frac{\partial T}{\partial r}\right)_{r=r_w} = \hat{q}t \tag{20}$$

we obtain

$$T_w - T = \hat{q}t\psi/2\pi k_f r_w. \tag{21}$$

The modified solution for the ideal line-source subjected to a ramp input, to correct first-order is

$$\Delta T_w = \Delta T + (T_w - T) = \frac{\hat{q}t}{4\pi k_f}\left[\ln\left(\frac{4\alpha t}{r_w^2 D}\right) + \frac{2\psi}{r_w}\right]. \tag{22}$$

Equation (22) shows that the principal effect of the Knudsen temperature jump is to shift the curve of $\Delta T/t$ vs $\ln t$ without changing its slope. Secondary effects will be much less than 0.3% since the gradual temperature increase in wire results in a negligible temperature jump even at low densities.

4.6. *Axial conduction*

Heat is lost from the wire both radially to the surrounding fluid, and axially to the supporting ends. The axial conduction effect therefore results in a modification of the transient temperature profile of the ideal line-source since the profile becomes a function of both axial position and time. In order to determine the effect of this modified temperature profile and the thermal conductivity of the fluid, a comparison is made between a finite length of a fine wire bounded by infinite conducting media at both ends, and a finite length of an infinitely long wire.

Consider a perfectly cylindrical wire with a finite length bounded by two infinite conducting media. The wire is heated internally due to the passage of a current I and is cooled by loss of heat to the surrounding fluid with an interfacial conductance coefficient H_0, which for simplicity is assumed to be constant. (Note that in the real situation $H_0 = f(T)$.) Heat is also lost to both ends through the axial conduction mechanism. One can obtain an indication of the importance of axial conduction by comparing the solutions for the infinite wire and the bounded wire.

The governing differential equation and boundary conditions for this idealized situation, in dimensionless form, are as follows

$$\frac{\partial\theta_w}{\partial\tau_w} = \frac{\partial^2\theta_w}{\partial Z^2} - H(\theta_w - \theta_f) + Q \tag{23}$$

with boundary conditions

$$\theta_w = 0 \quad \text{at} \quad \tau_w = 0$$

$$\theta_w = 0 \quad \text{at} \quad Z = 0 \quad \text{and} \quad Z = L/r_w.$$

The solution to the above differential equation for a ramp heat input perturbation is given by

$$\theta_w(Z,t) = \frac{\hat{q}t}{T_0 H_0 P}\left[1 - \frac{\sinh\mu Z + \sinh\mu(L-Z)}{\sinh\mu L}\right] - \frac{4\hat{q}L^2\mu^2}{\pi H_0 P T_0}\sum_{n=1}^{\infty}\left[[1-\exp(-A_n t)]\left(\frac{B_n}{C_n A_n}\right)\right] \tag{24}$$

where $A_n = H + \alpha_w(2n-1)^2\,(\pi/L)^2$; $B_n = \sin[(2n-1)\pi Z/L]$; and $C_n = (2n-1)\,[(2n-1)^2\mu^2 + L^2\mu^2]$.

In the case of the infinite line-source with axial conduction, the transient temperature profile is described by

$$\frac{\mathrm{d}\theta_w}{\mathrm{d}\tau_w} = Q - H\theta_w \tag{25}$$

with boundary condition

$$\theta_w = 0 \quad \text{at} \quad \tau_w = 0.$$

The solution to the above differential equation for a ramp heat input is given by

$$\theta_w(t) = \frac{\hat{q}r_w^2}{H_0 P T_0 \alpha_w}\left[\tau_w - \frac{1}{H}(1 - \mathrm{e}^{-Ht})\right]. \tag{26}$$

The integral average wire temperature at time t is defined by the following equation

$$\bar{\theta}_w(t) = \int_0^{L/r_w} \theta_w(Z,t)\,\mathrm{d}Z. \tag{27}$$

Equation (24) was numerically evaluated with different parameters comparable to typical experimental cases. The differences between the thermal conductivity obtained using $\bar{\theta}_w$ and the one using θ_w was found to be negligible, for a typical experiment, using a wire with radius 6.35 μm and length greater than 0.1 m. For shorter wires the error was larger, though still negligible (i.e. for $L = 0.05$ m, error in slope, 0.16%). For design purposes, the error due to axial conduction for a wire with a radius in the order of 6.35 μm is negligible for any length greater than 0.10 m. For very accurate measurements one might utilize the well-established experimental technique of employing a compensating wire to reduce the predicted error by orders of magnitude. Details of this technique and the appropriate working equations are presented by de Castro *et al.* [18], and by Anderson *et al.* [19].

4.7. *Free convection*

In previous studies the onset of convection has been estimated for a finite length of a semi-infinite vertical wire subjected to a step change in heat input. It has been shown [20] that the initial part of the transient is locally pure conduction with a transient one-dimensional temperature field. This regime is terminated at any particular point in the vertical coordinate, by the leading edge of the fluid molecules moving upward with velocities determined from the one-dimensional analysis. Mani [9] has estimated the maximum penetration distance of the leading edge effect for a step change in heat flux for both one-dimensional and two-dimensional cases. Other transient natural convection studies in relation to thermal conductivity measurements, have generally used the leading edge analogy [11]. Since the prediction of the thermal conductivity is based on the transient temperature profile at the wire–fluid interface, a more correct criteria for free convection effects should involve the transient integral average wire temperature. The experimental study of Pantaloni *et al.* [21] also suggests that the onset of convection is related to a vertical component of the thermal gradient. In the case of the ramp perturbation the dynamic process is governed by the following momentum and energy equations which are simplified by the Boussinesq approximation [22] and by the boundary-layer assumption

$$\frac{\partial U}{\partial \tau} + U\frac{\partial U}{\partial Z} + V\frac{\partial U}{\partial R} = \frac{1}{R}\frac{\partial}{\partial R}\left(R\frac{\partial U}{\partial R}\right) + Gr\,\theta \quad (28)$$

$$\frac{\partial \theta}{\partial \tau} + U\frac{\partial \theta}{\partial Z} + V\frac{\partial \theta}{\partial R} = \frac{1}{Pr}\frac{1}{R}\frac{\partial}{\partial R}\left(R\frac{\partial \theta}{\partial R}\right) \quad (29)$$

$$\frac{\partial U}{\partial Z} + \frac{\partial V}{\partial R} + \frac{V}{R} = 0. \quad (30)$$

Initial and boundary conditions are:

$$U = V = \theta = 0 \begin{cases} \text{for all } R \text{ and } Z,\ \tau \leqslant 0 \\ \text{at } Z = 0, \text{ all } R,\ \tau > 0 \\ \text{at } R \to \infty, \text{ all } Z,\ \tau > 0 \end{cases}$$

$$U = V = 0, \text{ at } R = 1 \text{ for all } Z,\ \tau > 0$$

$$-\left.\frac{\partial \theta}{\partial R}\right|_{R=1} = \frac{\hat{Q}}{2\pi}, \quad \text{all } Z,\ \tau > 0.$$

These conditions are consistent with previous studies [9] and only differ on the forcing function. A numerical solution to the partial differential equations (PDES) was developed based on the method of lines for one spatial variable and forward difference for the second spatial variable. The method of lines uses a finite element collocation procedure with piecewise polynomials as the trial space for the descretization of the spatial variable [23]. The forward difference procedures reduce the PDE system to a number of PDES in one spatial variable which are then reduced to a semi-discrete system of ordinary differential equations which only depend on time. The time integration is then accomplished by use of slightly modified standard techniques [24, 25].

The temperature profiles are obtained as

$$\theta = f(R, Z, \tau)$$

and the integral average temperature profile at the wire surface is obtained as

$$\bar{\theta}_w(R, \tau) = \int_0^Z \theta\, dZ/Z\,|_{R=1} \quad (31)$$

from the ideal line source model a plot of θ/τ vs $\ln\tau$ gives a straight line with its slope proportional to the thermal conductivity. It is expected that a similar plot using $\bar{\theta}_w$ as the wire temperature will give a straight line at short times and will show a change to a lesser slope at the onset of convection. A plot of $\bar{\theta}_w/\tau$ vs $\ln\tau$ for a typical case of methane at 300 K and 5.0 MPa is shown in Fig. 4. As it is seen, at short times a straight line is obtained. The criterion for onset of convection is determined by deviation from linearity of by more than 0.1 % (change in slope). This point is defined as τ^* on Fig. 4. By varying the slope of the ramp, Prandtl and Grashof numbers a series of curves representing the time for the onset of convection as a function of dimensionless heat parameter Q^* are developed and are presented in Fig. 5. The dimensionless heat parameter Q^* is equivalent to $\theta Nu^*/\tau Nu$ where Nu^* and Nu are Nusselt numbers; the former is based on the radius of the wire, and the latter is based on the thermal boundary layer thickness. These curves, in the order of increasing Rayleigh number represent methane at 300 K and 5.0 MPa, toluene at 300 K and 0.1 MPa, and SRC-II (coal derived) naphtha No. 1046 at 310.8 K and 0.1 MPa, respectively.

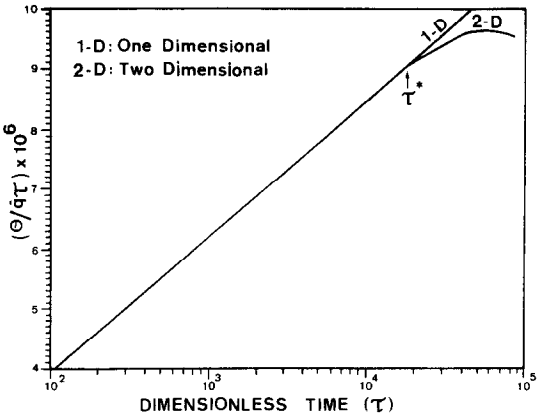

FIG. 4. Separation of the transient two-dimensional from transient one-dimensional solutions in a ramp forced system.

By specifying the slope of the ramp $\hat{q}$, and the physical parameters of the system, one can obtain the time for the onset of convection from Fig. 5. The temperature rise of the wire at the time of the onset of convection can be obtained from Fig. 6 which is a graphical presentation of the ideal line-source solution for different Prandtl numbers. A more simplified method of presenting the onset of convection can be shown in terms of a modified Rayleigh number which expresses the transient radial temperature profile as follows:

$$R_a(t) = [(\beta g/\nu\alpha)]\delta_t^3 \Delta T(r, t). \quad (32)$$

The thermal boundary layer thickness is assumed to be given by

$$\delta_t = \phi\sqrt{(\alpha t)} \quad (33)$$

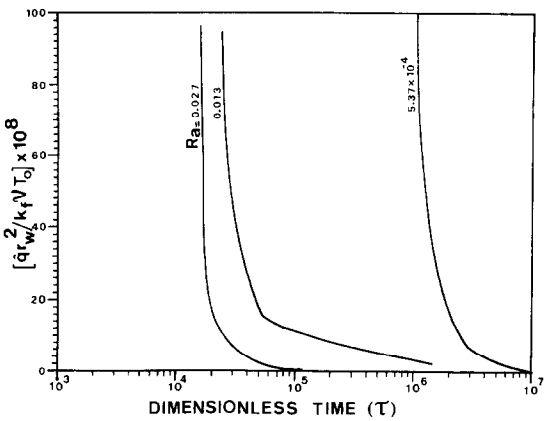

FIG. 5. Onset of convection in a medium surrounding a vertical line source subjected to a ramp heat input perturbation.

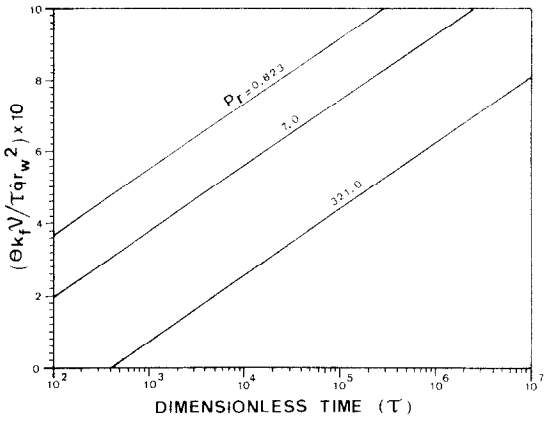

FIG. 6. Transient one-dimensional conduction in a thermal conductivity cell subjected to a ramp heat input perturbation — the effect of Prandtl number.

where ϕ is a numerical factor. By substituting equation (10) in equation (32) we obtain

$$R_a(t) = \left[\frac{\phi^3 \beta g \alpha^{1/2}}{\nu}\right]\left[\frac{\hat{q}}{4\pi k_f}\right] t^{5/2} \ln\left[\frac{4\tau}{DP_r}\right]. \quad (34)$$

According to Pantaloni *et al.* [21], the experimental values for the onset of convection from a vertical wire immersed in three different liquids and heated with a step change, resulted in a unique value of the Rayleigh number [i.e. $R_a(t^*) \sim 30\phi^3$]. Pantaloni did not extend this analysis to vapors and gases.

For the ramp heat input, the free convection equations result in approximate Rayleigh numbers defined by equation (32), of $58\phi^3$, for liquids and $390\phi^3$ for methane gas. Furthermore, a strong dependency of the Rayleigh number on $\hat{q}$ at low heat input levels is observed. These observations suggest that the use of the modified Rayleigh number with a constant numerical factor is insufficient in describing the transient behavior in a ramp forced system. Referring back to Fig. 5, the obtained Rayleigh numbers of ($58\phi^3$) and ($390\phi^3$), approximately describe the intermediate region (i.e. $20 \times 10^{-8} < Q^* < 80 \times 10^{-8}$). Substituting these Rayleigh numbers in equation (34) yields equation (35)

$$t^{*5/2} \ln\left[\frac{4\alpha t^*}{r_w^2 D}\right] = \xi Pr \alpha^{1/2} (k_f/\beta g \hat{q}) \quad (35)$$

where $\xi = 730$ for liquids and $\xi = 4900$ for gases.

As an example, equation (35) with heat input at a rate of 566 mW m^{-1} s^{-1} gives a time for the onset of convection for methane, toluene and SRC-II naphtha as 0.7 s, 1.7 s and 7.3 s, respectively. Experimental results of Pantaloni *et al.* [21] for the same overall heat input for a step function gives a time for the onset of convection of 1.3 s for toluene.

As a result of this analysis a typical set of operating parameters for thermal conductivity measurement are presented in Table 4.

4.8. *Radiation effects*

Physically some of the energy is radiated away from the hot wire due to the temperature difference between the wire and surroundings. The radiated energy is partly absorbed by the fluid, whose absorptivity is strongly selective with respect to wave length and partly absorbed and re-emitted from the outer cylinder. In the case of a step change in heat input, Mani [9] has presented a complete analysis of approximations of the radiation contribution to the apparent thermal conductivity.

Radiation effects of a ramp heat input to the wire can be obtained by modification of the step heat input analysis.

Conservation of energy in a stationary radiation-participating medium in local thermodynamic equilibrium is described by equation (36)

$$\rho C_p \frac{\partial T}{\partial t} = -\operatorname{div} q \quad (36)$$

where

$$q = q_c + q_r$$

q_c and q_r represent the conductive and radiative contributions, respectively.

In evaluating q_r, three different radiative regimes should be considered:

(a) *Perfectly opaque fluid*: the radiative component $q_r = 0$, and therefore, no correction is required.

(b) *Transparent fluid*: the amount of energy radiated is given by Horrocks and McLaughlin [26] and simplified by Healy *et al.* [12] as

$$q_r = 2\pi r_w \sigma (T_w^4 - T_0^4) \simeq 8\pi r_w \sigma T_0^3 \Delta T_w. \quad (37)$$

The radiation loss modifies the lines source solution and is equivalent to a reduction in $T(r_w, t)$ by the amount.

$$\delta T = \frac{(q_r)}{q} \Delta T(r_w, t) = \frac{8\pi r_w \sigma T_0^3}{\hat{q}t} [\Delta T(r_w, t)]^2. \quad (38)$$

The above conditions are satisfied in measurements on dilute gases in the thermal conductivity cell. The correction is negligible due to small temperature differences and small radius of the wire.

(c) *Partially absorbing fluid*: in this case the heat is absorbed by the fluid depending on its optical thickness $\bar{\tau}_0$ which is defined by the relation

$$\bar{\tau}_0 = K_a E \quad (39)$$

where K_a is the mean extinction coefficient for radiation and E is a characteristic dimension. The mean extinction coefficient is defined by

$$K_a = \int_0^\infty K_\S I_\S(T) d\S \Big/ \int_0^\infty I_\S(T) d\S \quad (40)$$

where $I_\S$ is the black body radiation intensity for the frequency $\S$ and $K_\S$ is the extinction coefficient for this frequency.

Table 4. Simulated parameters for the thermal conductivity measurement in a ramp forced system

Fluid	T_0 K	P, MPa	$\hat{q}$, W m^{-1} s^{-1}	t^*, s	ΔT^*, K
Methane	300	5.0	0.03	2.1	1.4
			0.07	1.5	2.2
			0.566	0.7	7.6
Toluene	300	0.1	0.40	2.0	4.1
			0.566	1.7	4.8
			0.80	1.5	5.9
SRC-II	300	0.1	0.10	14.5	8.9
			0.20	11.0	13.1
			0.566	7.3	23.6

$r_w = 6.35 \times 10^{-6}$ m.

4.9. *Optically thick approximations*

For a strongly absorbent fluid ($\bar{\tau}_0 \gg 1$) the radiative transfer can be treated as a diffusional process

$$q_r = -k_r \operatorname{grad} T$$

where q_r is independent of the cell geometry and k_r is constant which depends on the optical properties of the fluid. Poltz's [27] expression for q_r in an optically thick plane parallel layer is valid for the present cell configuration

$$q_r = \left[\frac{16\eta^2}{3\kappa}\sigma T_0^3\right]\operatorname{grad} T \tag{41}$$

and

$$k_r = \frac{16\eta^2}{3\kappa}\sigma T_0^3. \tag{42}$$

The solution of the energy with ramp perturbation can be simplified as

$$\frac{\theta}{t} = \frac{\hat{q}}{4\pi k_f(1+A)}\left[\ln\frac{4\alpha t(1+A)}{r_w^2 D} + \ldots\right] \tag{43}$$

where $A = q_r/q_c$.

It can be shown that for strongly absorbent fluids the apparent thermal conductivity may increase to about 8% above its radiation-free value.

4.10. *Optically thin approximation*

For $\bar{\tau}_0 \ll 1$, there is negligible self-absorption and ths fluid exchanges radiation directly with the bounding surfaces and not with itself. The influence of the bounding surfaces is more pronounced in the parallel plate or co-axial cylindrical geometry than in a hot-wire method. The surface area of the emitter is small compared to the volume of the thermally disturbed fluid and the medium beyond the boundary layer and the outer wall act as black bodies.

The optically thin approximation is similar to the transparent regime assumption in the hot-wire cell and hence negligible correction.

4.11. *Intermediate regime*

In this regime each fluid element exchanges radiation with other fluid elements as well as with the bounding surfaces. The fluid adjacent to the wire though absorbs radiation emitted by the wire surface receives back only a small proportion of its own emitted radiation unlike the fluid away from the wire. Therefore, at large values of time and for small Bouguer number ($BU = \kappa r_w \ll 1$) (28), the fluid close to the wire is always optically thin, away from the wire it is optically thick, with transition in the intermediate region. The radiant heat flux at the wire is approximated as

$$A = \left.\frac{q_r}{q_c}\right|_{r_w} = \left[\frac{16\eta^2 r_w \sigma T_0^3}{\pi k_f}\right]\bar{R}(t, K_a, r_w, \varepsilon). \tag{44}$$

Values of $\bar{R}$ have been approximated by Mani [9] and by Saito and Venart [29]. Aside from the basic assumptions of small radiative contribution, grey body absorption, and additive radiative and conductive fluxes, these analyses differ in two respects. Mani's analysis of the internal zone is algebraic and based on an optically thin limit, whereas Saito and Venart's solution is numerical using a modified integral method without this assumption. Furthermore Mani assumed that the emissivity of platinum was unity. Based on the above discussion, it is evident that the numerical values of $\bar{R}$ differ in both analyses. Since all transient hot-wire cells are fitted with a platinum wire (emissivity 0.037), the Saito and Venart analysis for evaluation of $\bar{R}$, is more appropriate.

Rearranging equation (43) we get

$$\frac{\theta}{t} = \frac{\hat{q}}{4\pi k_f}\ln(4\alpha t(1+A)/r_w^2 D)^{1/1+A}. \tag{45}$$

A plot of θ/t vs $\ln(1+A)t^{1/1+A}$ gives the radiation free value of the thermal conductivity.

For similar heat input to the wire, at short times when the temperature rise for a ramp forced wire is considerably less than the one for a step forced case, the radiative contribution will be considerably less. At large times, however, the radiative contribution may become higher for the ramp depending on the actual temperature difference.

Typically for toluene at 25°C ($\eta = 1.5, \kappa = 35\,\text{cm}^{-1}$) the radiative contribution to the apparent thermal

conductivity is 0.3%. The radiative correction increases at higher temperatures and longer times. This suggests that a radiation free value for the thermal conductivity can be obtained by extrapolating the obtained time variant thermal conductivity values to time zero.

In conclusion, it is apparent from the above discussion that a radiative correction in a typical thermal conductivity cell is only needed for fluids with moderate and high optical thicknesses and then only if the maximum temperature rise exceeds 2–3 K.

SUMMARY

Three heat generation forcing functions (step, Dirac, and ramp) for use in the transient thermal conductivity technique are evaluated. It is shown that the ramp function offers several advantages over the step and Dirac functions. For the idealized model of a vertical line source subjected to a ramp perturbation source the thermal conductivity is obtained from the slope of the $\Delta T/t$ vs $\ln t$ diagram. Analytical and/or numerical solutions to the deviations from the ideal line-source model for the ramp have been given. These include truncation error, non-uniform wire radius, heat capacity effect, bounded media, Knudsen effects, axial conduction, free convection and radiation. These deviations can be used to design a ramp driven thermal conductivity system such that negligible corrections to the raw experimental data need be made. Therefore, with appropriate cell design, the thermal conductivity can be deduced directly from the ideal line-source model. Work currently underway to apply these results will be reported in a separate article.

Acknowledgements—We gratefully acknowledge the support of the Department of Energy under contract DE-AC02-79ER10393 and the assistance of Professors M. C. Jones and R. A. Walsh.

REFERENCES

1. J. Hirshfelder, C. F. Curtis and R. B. Bird, *Molecular Theory of Gases and Liquids*. Wiley, New York (1954).
2. J. J. DeGroot, J. Kestin and H. Sookiazian, Instrument to measure the thermal conductivity of gases, *Physica, 's Grav.* **75,** 454–482 (1974).
3. A. A. Clifford, J. Kestin and W. A. Wakeham, Thermal conductivity of N_2, CH_4 and CO_2 at room temperature and at pressures up to 35 MPa, *Physica, 's Grav.* **97A,** 287–295 (1979).
4. J. Kestin and W. J. Wakeham, A contribution to the theory of the transient hot-wire technique for thermal conductivity measurements, *Physica, 's Grav.* **92A,** 102–116 (1978).
5. J. J. DeGroot, J. Kestin and H. Sookiazian, The thermal conductivity of four mono-atomic gases as a function of density near room temperature, *Physica, 's Grav.* **92A,** 117–144 (1978).
6. C. A. Nieto de Castro, J. C. G. Calado, W. J. Wakeham and M. Dix, An apparatus to measure the thermal conductivity of liquids, *J. Phys. E.* **9,** 1073 (1976).
7. W. N. Trump, H. W. Luebke, L. Fowler and E. M. Emergy, Rapid measurement of liquid thermal conductivity by the transient hot-wire method, *Rev. Scient. Instrum.* **48,** 47 (1977).
8. P. S. Davis, F. Theeuwes, R. J. Bearman and R. P. Gordon, Non-steady-state, hot-wire thermal conductivity apparatus, *J. Chem. Phys.* **55,** 4776 (1971).
9. N. Mani, Precise determination of the thermal conductivity of fluids using absolute transient hot-wire technique, Ph.D. Dissertation. University of Calgary, Alberta, British Columbia (1971).
10. H. S. Carslaw and J. C. Jaeger, *Conduction of heat in solids*, p. 158. Oxford University Press, Oxford (1959).
11. E. McLaughlin and J. F. T. Pittman, Determination of the thermal conductivity of toluene – A proposed data standard – from 180 to 400 K under saturation pressure by the transient hot-wire method I. The theory of the technique, *Phil. Trans. R. Soc.* Series A, 557 (1971).
12. J. J. Healy, J. J. DeGroot and J. Kestin, The theory of the transient hot-wire method for measuring thermal conductivity, *Physica, 's Grav.* **82C,** 392–408 (1975).
13. J. Fischer, *Ann. Phys.*, LPZ **34,** 669 (1939).
14. V. S. Arpaci, *Conduction heat transfer*. Addison-Wesley (1966).
15. *Handbook of mathematical Functions*, (edited by M. Abramwitz and I. A. Stegnn). Dover, New York (1965).
16. *Royal Society Mathematical Tables*, Vol. 7, *Bessel Functions* Part III, (edited by F. W. J. Olver). Cambridge University Press, Cambridge (1960).
17. M. Smoluchowski, *Ann. Phys. Chem.* **35,** 983 (1911).
18. C. A. Nieto de Castro, J. C. G. Calado and W. J. Wakeham, Thermal conductivity of organic liquids measured by a transient hot-wire technique, high temperatures–high pressures, **11,** 551–559 (1979).
19. G. P. Anderson, J. J. DeGroot, J. Kestin and W. A. Wakeham, *J. Phys. E.* **7,** 948 (1974).
20. R. Siegel, Transient free convection from a vertical flat plate, *Trans. Am. Soc. Mech. Engrs. J. Heat Transfer* **8D,** 347 (1958).
21. J. Pantaloni, E. Guyon, M. G. Velarde, R. Bailleux and G. Finiels, The role of convection in the transient hot-wire method, *Revue de Physique Appliquée* **12,** 1849 (1977).
22. J. M. Milhaljan, A rigorous exposition of the Boussinesq approximation applicable to a thin layer of fluid, *A.P.J.* **136,** 1126 (1962).
23. R. F. Sincorec and N. K. Madsen, Software for nonlinear partial differential equations, *ACM Toms* 1, No. 3, 232–260 (1975).
24. A. C. Hindmarsh, Preliminary documentation of GEARIB solution of implicit systems of ordinary differential equations with banded Jacobians. Lawrence Livermore Lab., UCID 30130 (1976).
25. C. Deboor, Package for calculating with B-splines, *SIAM J. Numer. Anal.* **14,** No. 3, 441–472 (1977).
26. J. Horrocks and E. McLaughlin, Temperature dependence of the thermal conductivity of liquids, *Trans. Faraday Soc.* **59,** 1709 (1963).
27. H. Poltz, Thermal conductivity of liquids – II. The radiation portion of the effective thermal conductivity, *Int. J. Heat Mass Transfer* **8,** 515 (1965).
28. G. Emanuel, Radiative energy transfer from a small sphere, *Int. J. Heat Mass Transfer* **12,** 1327 (1969).
29. A. Saito and J. E. S. Venart, *Proceedings of the Sixth International Heat Transfer Conference* (National Research Council of Canada), 3, 79–84 (1978).

MODELE MATHEMATIQUE D'UN INSTRUMENT DE CONDUCTIVITE THERMIQUE A FIL CHAUFFE SELON UNE RAMPE

Résumé—On étudie le modèle fondamental et ses corrections pour la détermination absolue de la conductivité thermique de fluide à partir de la technique du fil chaud en régime variable. On présente des solutions analytiques pour trois fonctions de génération de chaleur (Dirac, échelon, rampe). La fonction rampe offre plusieurs avantages sur la fonction échelon qui est courrament utilisée par les expérimentateurs. Des expressions pour les corrections du modèle idéalisé d'un système avec rampe sont présentées en ce qui concerne: l'effet de capacité thermique, l'erreur de troncature, le rayon non uniforme du fil, les frontières du milieu, l'effet Knudsen, la conduction axiale, la convection libre et le rayonnement.

EIN MATHEMATISCHES MODELL FÜR EIN HITZDRAHT-WÄRMELEITFÄHIGKEITSMESSGERÄT, DESSEN AUFHEIZUNG NACH EINER RAMPENFUNKTION VERLÄUFT

Zusammenfassung—Es wurden das Grundmodell sowie Modellkorrekturen zur absoluten Bestimmung der Wärmeleitfähigkeiten von Flüssigkeiten mittels einer instationären Hitzdrahtemethode untersucht. Analytische Lösungen für die Wärmeerzeugungsfunktionen (Einheitsimpuls, Sprung, Rampe) werden angegeben. Die Aufheizung nach der Rampenfunktion hat mehrere Vorteile gegenüber der Sprungfunktion, die allgemein von den Experimentatoren angewandt wird. Es werden Ausdrücke für die Korrekturen des idealisierten Modells eines mit der Rampenfunktion betriebenen Systems angegeben, und zwar für den Einfluß der Wärmekapazität, des Abbruchfehlers, ungleichförmigen Drahtdurchmessers, endlicher Medien, der Knudsen-Effekte, axialer Leitung, freier Konvektion und Strahlung.

МАТЕМАТИЧЕСКАЯ МОДЕЛЬ ИЗМЕРИТЕЛЯ ТЕПЛОПРОВОДНОСТИ, ПОСТРОЕННОГО НА ОСНОВЕ МЕТОДА НАГРЕТОЙ НИТИ, НА КОТОРУЮ ПОДАЕТСЯ ПИЛООБРАЗНОЕ НАПРЯЖЕНИЕ

Аннотация — Исследовалась модель, разработанная для определения теплопроводности жидкости нестационарным методом нагретой нити. Представлены аналитические решения для трех функций тепловыделения (функции Дирака, ступенчатой и пилообразной). Показано, что пилообразная функция тепловыделения имеет некоторые преимущества над ступенчатой, обычно используемой экспериментаторами. Представлены выражения для определения поправок к идеализированной пилообразной модели, которые учитывают: эффект теплоемкости, ошибку вследствие отбрасывания членов уравнения, неоднородность нити по радиусу, ограниченность среды, эффекты Кнудсена, аксиальную теплопроводность, свободную конвекцию и излучение.